An adsorptive solar ice-maker dynamic simulation for north Mediterranean climate

AN ADSORPTIVE SOLAR ICE-MAKER DYNAMIC SIMULATION FOR NORTH MEDITERRANEAN CLIMATE

S. Vasta[a], G. Maggio[a,*], G. Santori[b], A. Freni[a], F. Polonara[b], G. Restuccia[a]

[a]*CNR - Istituto di Tecnologie Avanzate per l'Energia "Nicola Giordano", Via Salita S. Lucia sopra Contesse 5, 98126 Santa Lucia, Messina, Italy.*

[b]*Università Politecnica delle Marche, Facoltà di Ingegneria, Dipartimento di Energetica,Via Brecce Bianche, Monte Dago, 60131 Ancona, Italy.*

Abstract

This paper presents a model for dynamic simulation of an adsorptive ice-maker. The model describes the different phases of the thermodynamic cycle of the ice-maker components: solar collector, adsorbent bed, condenser and cold chamber (evaporator and water to be frozen). The adsorbent/adsorbate working pair is active carbon/methanol.

The simulations were performed for a whole year using measured climatic data of Messina (38° 12' N). The detailed results of a week of June and December 2005 are shown, as representative of typical summer and winter conditions. These simulations showed that the ice-maker is able to freeze 5 kg of water during all days of June, and, if the weather conditions are not too unfavourable, also during December. Further simulations, carried out for the whole year 2005, demonstrated that during the most part of the year (from April to October) a Daily Ice Production (DIP) of 5 kg can be obtained, and an Equivalent Daily Ice Production (DIP_{eq}) near to 5.5 kg can be reached.

[*] *Corresponding author. Tel.: +39-90-624243; Fax: +39-90-624247; E-mail: gaetano.maggio@itae.cnr.it.*

During the months of February and March the average monthly DIP is about 4 kg. Finally, for the coldest months (January, November and December) the DIP was 2.0-3.5 kg.

The average monthly Solar Coefficient Of Performance (COPs) varies from a minimum of about 0.045 (July) to a maximum of 0.11 (January), with an annual mean of 0.07.

Keywords: Adsorption cooling, solar ice-maker, climatic data, ice-maker simulation

Nomenclature

A_i	Heat transfer surface, m^2 (i=1-5, 9)
a_i, b_i	Constants for equilibrium equation of adsorbent/adsorbate (i=0-3) (see Eqs. 8 and 9)
c	Specific heat, J kg^{-1} K^{-1}
c_i	Constants for condensation/evaporation pressure (i=0-3) (see Eqs. 11a and 11b)
COPs	Solar Coefficient Of Performance
d_i	Constants for latent heat of condensation/evaporation (i=0-3) (see Eq. 12)
DIP	Daily Ice Production (kg)
I_β	Available solar radiation @ β=30°, W m^{-2}
K_i	Flag: 0 or 1 (i=1-3) (see Eqs. 2 and 6a-b)
L_a	Adsorbate latent heat of condensation/evaporation, J kg^{-1}
L_w	Water latent heat of solidification, $334.4 \cdot 10^3$ J kg^{-1}
m	Mass, kg
m_a	Initial adsorbate mass inside the evaporator, kg
m_w	Liquid water mass, kg
n	Solar collector area, m^2

p	Pressure, Pa
R	Gas constant for adsorbate, J $kg^{-1}K^{-1}$
T	Temperature, K
t	Time, s
t_{cycle}	Cycle time, s
U_i	Global heat transfer coefficient, W m^{-2} K^{-1} (i=1-9)
U_α, U_β	Global heat transfer coefficient, W m^{-2} K^{-1} (see Table 2)
w	Uptake, kg kg^{-1}

Greek letters

$(\tau\alpha)_{eff}$	Transmittance/absorptivity coefficient
ΔH	Adsorption/desorption enthalpy, J kg^{-1} (see Eq. 10)
ΔT	Variation of temperature, K
Δw	Variation of uptake, kg kg^{-1}

Subscripts

1	Solar collector/environment
2	Solar collector/adsorbent
3	Condenser/environment
4	Evaporator/liquid water
5	Environment/liquid water
6	Evaporator/phase-changing water
7	Evaporator/solid water
8	Environment/solid water
9	Evaporator/environment
a	Adsorbate

amb Ambient

c Condenser

eq Equivalent

ev Evaporator

ice Iced water

lw Liquid water

m Solar collector (i.e. metallic housing of the adsorbent material)

s Solid adsorbent material (dry)

w Water

β Tilt angle

Superscripts

C Closed ventilation windows

O Open ventilation windows

1. Introduction

Adsorptive machines driven by solar energy are cheap, simple and not polluting solutions for cold production in remote areas far from electric grid, but where the solar radiation is widely available [1, 2]. The operating principle of such machines is based on the reversible physical adsorption of vapour (e.g. water, methanol) on the surface of a porous solid (e.g. silica gel, activated carbon). An attractive application is the intermittent "adsorptive solar ice-maker", which consists of a small size adsorptive reactor connected or integrated into a solar collector for regeneration of the sorbent material during the day, and to an evaporator for ice production during the night.

Several authors carried out experimental and/or theoretical studies aimed to the development of efficient adsorptive solar adsorption systems.

Among the most interesting experimental works, Sumathy and Z.F. Li designed and tested in Hong Kong a solar adsorption ice-maker with a single flat-plate collector (0.92 m^2 exposed area), based on the activated carbon/methanol pair [3, 4]. From their experiments resulted that this system can produce 4-5 kg ice daily, with a solar COP of 0.10-0.12. These values are in good agreement with those reported by M. Li [5] for a similar flat-plate ice-maker tested in Shanghai: 3.5-4.5 kg of ice and a COP of 0.12-0.147, for a solar collector of 0.75 m^2. Anyanwu and Ezekwe [6] designed, constructed and tested in Nsukka, Nigeria, a flat-type solar adsorption refrigerator using the activated carbon/methanol pair, with effective exposed area of 1.2 m^2. They obtained a maximum solar COP of 0.02, but this low value was attributed to the "non-selective collector plate surface coating used". Hildbrand et al. [7] developed an adsorption refrigerator based on silica gel/water pair; the total solar collector area was 2 m^2. The experiments were carried out over a period of 68 days in Yverdon-les-Bains, Switzerland, and showed the significant influence of the environmental conditions on the system performance. The solar COP was between 0.12 and 0.23.

The prototype designs in [3-6] have been supported by simple mathematical models based on general energy balances and COP calculations. Instead, other models for simulation of the heat and mass transfer processes through the porous adsorbent bed of a solar-powered ice-maker, were proposed in [8-12]. In particular, Passos et al. [8] presented a model which accounts for the resistances to mass transfer in the pellets by a linear driving force equation. They calculated the solar collector temperature, the exchanged mass of methanol and validated the model by experimental results. Hu [9] simulated a tubular solar collector to be used in an intermittent non-valve solar powered activated carbon/methanol refrigerator. The calculated temperature and methanol concentration maps inside the collector tube, at different times of the day, were presented. Anyanwu et al. [10] modelled the refrigerator prototype presented in [6] to

study the influence of various parameters on COP. The parametric study revealed that the solar refrigerator performance strongly depended on the absorptivity of the collector surface coating material. A two-dimensional transient heat and mass transfer mathematical model has been proposed by M. Li and Wang [11] for a flat-plate solar collector of 1.5 m^2, calculating an ice production of 8 kg and COP of 0.125, in agreement with experiments. Day and Sumathy [12] used a model to study a solar adsorbent cooling system in which the adsorber is a metal tube packed with activated carbon/methanol pair and surrounded by a vacuum glass tube. This model, differently from those proposed in [8-11], accounted for the effects of non-uniform pressure distribution.

The works presented in [8-12] were mainly devoted to accurate modelling of the sorbent bed, but are not suitable to satisfactorily describe the other components of the ice-maker system; besides, they have been applied by simulating just one or two days. On the contrary, some models which accounted for the various system components have been proposed in [13-15]. In particular, Leite et al. [13] used a predictive model for a solar adsorption ice maker, obtaining an average net solar COP of 0.13 and 7-10 kg/day of ice production. Hu and Exell [14] developed a uniform pressure model to simulate the daily performance of a refrigerator with tubular flat-plate collector (1.01 m^2 effective area). The model has been used to evaluate the influence of some design parameters and operating conditions on the system performance. A maximum solar COP of about 0.080 has been calculated. Boubakri et al. used experimental data of two adsorptive flat-plate ice-makers tested in Agadir, Morocco, to study by model [15] the performance sensitivity with respect to various physical parameters of the units. They obtained an average ice production of 5-6 kg m^{-2} for a system based on activated carbon AC-35/methanol pair.

Also these models considered climatic conditions for a short period, with the exception of Leite et al. [13], but they limited their investigation to "the hottest six months in João Pessoa, Brazil".

In this paper, a new mathematical model has been developed with the following aims: a) simulate a whole ice-maker system and calculate the descriptive parameters (e.g. adsorbent, solar collector, condenser and evaporator temperature; adsorbent pressure; methanol uptake; etc.) and performance parameters, as a function of real climatic conditions; b) evaluate the performance of the ice-maker for a period as long as a whole year. Therefore, this represents an innovative contribution to the current state-of-art, because the proposed model is a useful tool to accurately simulate the operation of all ice-maker components and determine the system performance – in terms of COPs, DIP and DIP_{eq} – for a whole year of continuous operation. Such features have not been reported in previous works.

The model is based on energy balances for the adsorbent reactor and the connected heat exchangers. The climatic data used as input parameters were experimentally recorded by means of a meteo-station installed at the CNR-TAE Institute in Messina. Values of solar radiation and ambient temperature taken every ten minutes for the whole year 2005, were used to perform the simulations.

2. Operating principle

An adsorptive solar ice-maker is made of the following components: a solar collector, in which the adsorbent material (active carbon) is embedded; a condenser for the adsorbate (methanol) condensation and its heat rejection to the ambient during the day; a "cold chamber", containing the evaporator and the liquid water to be frozen during the night. A scheme is presented in Figure 1.

During the day, the solar energy received by the collector allows the desorption of methanol from the sorbent bed. The methanol vapour flows to the condenser, condenses, and is collected inside a receiver. During the above described phase all valves are closed. In the late afternoon the valve V_1 (see Fig. 1) is opened, so that the liquid methanol flows from the receiver to the evaporator. Then, the valve V_1 is closed and the valve V_2 is opened for the whole night, allowing adsorption of methanol. The evaporation of methanol inside the cold chamber cools down the liquid water which is converted to ice.

From the thermodynamic point of view, the active carbon/methanol working pair follows the classic adsorptive cycle made of four phases: I) isosteric heating from p_{ev} to p_c (line AB in Fig. 2); II) desorption at high temperature and pressure of condensation (line BC); III) isosteric cooling at closed volume from p_c to p_{ev} (line CD); IV) adsorption at low temperature and pressure of evaporation (line DA). More details on the thermodynamic cycle of adsorptive machines can be found elsewhere [16].

3. Modeling and design

3.1 Model assumptions, equations and numerical solution

Figure 3 shows the control volume considered for the model formulation. As already mentioned, it consists of the three main elements of the ice-maker: the solar collector which holds the adsorbent material, the condenser and the cold chamber. In this figure, the symbols and values used for the model parameters are also indicated (see nomenclature).

The model is based on the following assumptions:

- All components are spatially isothermal and isobaric. Thus, the temperature of the adsorbent material and those of the system components do not vary spatially, but only temporally.

- The resistances to the methanol diffusion through the adsorbent bed and through the components are neglected.
- The adsorbent particles have uniform size, shape and distribution.
- In the adsorbent bed, the solid phase is in local thermal equilibrium with the gaseous phase.
- The gaseous phase behaves as an ideal gas.
- All specific heats of the components and the heat transfer coefficients are assumed to be constant.
- The thermal losses along the pipes are neglected.

The model is based on heat balance equations for the solar collector, the embedded adsorbent bed, the condenser and evaporator.

Solar collector:

$$n(\tau\alpha)_{eff} I_\beta = m_m c_m \frac{dT_m}{dt} + U_2 A_2 (T_m - T_s) + U_1^{C/O} A_1 (T_m - T_{amb}) \quad \textbf{(1),}$$

Adsorbent bed:

$$U_2 A_2 (T_m - T_s) = (m_s c_s + w m_s c_a) \frac{dT_s}{dt} - K_1 m_s \Delta H(w) \frac{dw}{dt} \quad \textbf{(2)},$$

Condenser:

$$L_a(T_c) m_s \frac{dw}{dt} = -m_c c_c \frac{dT_c}{dt} - U_3 A_3 (T_c - T_{amb}) \quad \textbf{(3a),}$$

Evaporator:

$$L_a(T_{ev}) m_s \frac{dw}{dt} = -U_\alpha A_4 (T_{ev} - T_w) - [m_{ev} c_{ev} + (m_a - \Delta w m_s) c_a] \frac{dT_{ev}}{dt} - U_9 A_9 (T_{ev} - T_{amb}) \quad \textbf{(3b).}$$

The following additional heat and mass balance equations allow to simulate the cold chamber operation.

Water/ice heat and mass balances:

$$m_w c_w \frac{dT_w}{dt} = U_\alpha A_4 \left(T_{ev} - T_w\right) + U_\beta A_5 \left(T_w - T_{amb}\right) \quad \textbf{(4),}$$

$$L_w \frac{dm_{ice}}{dt} = L_a \left(T_{ev}\right) m_s \frac{dw}{dt} \quad \textbf{(5).}$$

As usual for most engineering applications, the governing equations used in the proposed analysis are based on the energy conservation and the rate equations [17], both consistent with our model assumptions. In particular, in equations (1)-(4), the term $n(\tau\,\alpha)_{eff}\, I_\beta$ is the thermal power coming from the solar radiation; the terms of the form $m\,c\,\frac{dT}{dt}$ are sensible heats; the terms of the form $U\,A\,\Delta T$ represent the heat rates, involving the global (convection and conduction) heat transfer coefficients; $m_s \Delta H(w) \frac{dw}{dt}$ is a source term due to adsorption/desorption; and the terms $L(T)\, m \frac{dw}{dt}$ are latent heats. Finally, equation (5) allows to determine the mass of liquid water converted into ice; it assumes that the cold (latent heat) derived from methanol evaporation produces the water freezing.

The model allows calculation of the dynamic behaviour of the temperature, in the various components of the machine, as well as, the adsorbent pressure, the methanol uptake and the production of ice. Furthermore, for each day, the corresponding Solar Coefficient Of Performance (COPs) is calculated as the ratio between the useful effect and the available solar energy:

$$COPs = \frac{Useful\ effect}{Available\ solar\ energy} = \frac{m_w\, c_{lw}\, \Delta T_w\big|_{step\ IVa} + K_2\, m_{ice}\, L_w + K_3\, m_w\, c_{ice}\, \Delta T_w\big|_{step\ IVc}}{n \int_0^{t_{cycle}} I_\beta(t)\, dt} \quad \textbf{(6a),}$$

where K_2=0 and/or K_3=0 when Step IVb and/or IVc does not occur (see below for step's description).

The Daily Ice Production (DIP) and its equivalent value (DIP_{eq}), which accounts for the ice corresponding to the under-cooling, are given by

$$DIP = K_2\ m_{ice} \qquad \text{and} \qquad DIP_{eq} = DIP\left(1 + \frac{m_w\ c_{ice}\ \Delta T_w\big|_{step\ IVc}}{m_{ice}\ L_w}\right) \qquad \textbf{(6b-c).}$$

Supplementary equations are reported below.

- The adsorbent/adsorbate equilibrium was calculated by the following equation [18]:

  $$ln(p_s) = A(w) + \frac{B(w)}{T_s} \qquad \textbf{(7),}$$

  where the terms $A(w)$ and $B(w)$ are polynomials

  $$A(w) = a_0 + a_1\ w + a_2\ w^2 + a_3\ w^3 \qquad \textbf{(8),}$$

  $$B(w) = b_0 + b_1\ w + b_2\ w^2 + b_3\ w^3 \qquad \textbf{(9).}$$

- The adsorption/desorption enthalpy $\Delta H(w)$ appearing in equation (2) was calculated as

  $$\Delta H(w) = -B(w)\,R \qquad \textbf{(10),}$$

  where R is the gas constant for adsorbate, which is about 259.5 J $kg^{-1}K^{-1}$ for methanol.

- The condensation/evaporation pressure is given by [19]

  $$ln(p_c) = c_0 + \frac{c_1}{T_c} + \frac{c_2}{T_c^2} + \frac{c_3}{T_c^3} \qquad \textbf{(11a),}$$

  $$ln(p_{ev}) = c_0 + \frac{c_1}{T_{ev}} + \frac{c_2}{T_{ev}^2} + \frac{c_3}{T_{ev}^3} \qquad \textbf{(11b).}$$

- The latent heat of condensation/evaporation of adsorbate, was calculated as a function of temperature by [19]

$$L_a(T) = d_0 + d_1\,T + d_2\,T^2 + d_3\,T^3 \qquad \textbf{(12).}$$

In particular, equation (7) describes the relationship between the pressure of the adsorbent, the adsorbent temperature and the uptake; while equations (11a) or (11b) allow to calculate the pressure of the adsorbent bed $p_s(t)$, as a function of the condenser/evaporator temperature.

The accompanying initial conditions and starting values are:

$$T_m(0) = T_s(0) = T_{amb}(0), \quad p_s(0) = p_{ev}, \quad w(0) = w_2 \qquad \textbf{(13a-c),}$$

$$T_c(t_1) = T_{amb}(t_1), \quad T_{ev}(t_3) = T_w(t_3) = T_{ev,0}, \quad m_{ice}(t_{4a}) = 0 \qquad \textbf{(13d-f),}$$

where p_{ev} is calculated from the initial evaporator temperature, w_2 is calculated from the initial temperature and pressure of the adsorber, t_1 is the time of end of Phase I (and start of Phase II), t_3 is the time of end of Phase III (and start of Step IVa), t_{4a} is the time of end of Step IVa (and start of Step IVb) and $T_{ev,0}$ (initial evaporator temperature) is an input data.

Depending on the phase of the thermodynamic cycle described by the adsorptive ice-maker, only a certain number of the previous equations (1)-(5) is valid and the relative coefficients/parameters (K_1, $U_1^{C/O}$, U_α, U_β, c_w) will assume a different form (see Tables 1-2).

Some details on the different phases are given below.

- *Phase I* (*isosteric heating*): The adsorbent is heated up along the upper isosteric curve (w=w_2=const), and the pressure increases from p_{ev} to p_c (line AB in Fig. 2). During this phase, the bed is not connected to the evaporator. The unknowns are $T_m(t)$, $T_s(t)$ and $p_s(t)$. The shift condition to the next phase is established

when $p_s=p_c$, i.e. when the adsorbent bed pressure reaches the condenser pressure.

- *Phase II* (*desorption*): When the condensation pressure of methanol is reached, the adsorbent bed is connected to the condenser. The adsorbent material releases the methanol, so that, the uptake varies between the upper and the lower isosteric curve (line BC in Fig. 2). The unknowns are $T_m(t)$, $T_s(t)$, $p_s(t)$, $w(t)$ and $T_c(t)$. The shift condition to the next phase is established when the useful solar radiation of the day drops below a certain value (I_β<100 W m^{-2}) or the methanol uptake is lower than 2%.
- *Phase III* (*isosteric cooling*): When one of the two above mentioned conditions occurs, the adsorbent bed is cooled down along the lower isosteric curve ($w=w_1=const$), through the opening of ventilation windows of the solar collector (line CD in Fig. 2). The unknowns are $T_m(t)$, $T_s(t)$ and $p_s(t)$. The shift condition to the next phase is established when $p_s=p_{ev}$, i.e. when the adsorbent bed pressure reaches the evaporator pressure.
- *Phase IV* (*adsorption*): Once the pressure p_{ev} is reached, the connection with evaporator is established and the methanol flows to the adsorbent. The uptake varies from the lower to the upper isosteric curve (line DA in Fig. 2). In the meantime, the methanol evaporation results in useful effect of water cooling. The water initial temperature (assumed to be 10 °C) decreases to 0 °C; then the liquid water undergoes a phase-change (ice) at constant temperature and finally it is under-cooled until the next day comes, or until the methanol contained in the evaporator is completely evaporated. During this phase, the unknown variables are $T_m(t)$, $T_s(t)$, $p_s(t)$, $w(t)$, $T_{ev}(t)$ and the temperature of the water $T_w(t)$ (or the mass of ice $m_{ice}(t)$, in the case of Step IVb).

Phase IV has been split into three steps, because the water may be at liquid phase (Step a), at solid/liquid mixture (phase-change; Step b) and at solid phase (Step c). Therefore, there are three distinct relationships (eq. (4) – with two different sets of values for the U_α, U_β, c_w coefficients – and eq. (5); see Table 2 for details).

The model equations were numerically solved by using a commercial software (Mathematica® 4.0 by Wolfram Research, [20]) for ordinary differential equation (ODE) systems, based on a function which automatically switches between stiff (Gear) and non-stiff (Adams) integration methods [21].

3.2 Adsorptive ice maker design

The design of the simulated adsorptive ice-maker is presented in Fig. 4. The flat-type solar collector has a surface area of 1.5 m^2 and contains 13 concentric tubes where the granular active carbon – about 37 kg – is embedded. The volume of the solar collector is about 0.5 m^3. The solar collector is equipped with ventilation windows which are closed during the day and opened during the night to enhance the dissipation of the adsorption heat. The condenser is a simple copper finned coil. The cold chamber contains a trapezoidal methanol evaporator [6] and 5 kg of water to be frozen. The volume of the whole ice-maker is about 7 m^3.

4. Results

4.1 Input data

The input data required by the model are reported in Fig. 3. Figure 5a-b shows, as an example, the values of the dynamic data (I_β and T_{amb}) for the mentioned typical summer (2-8 June 2005) and winter week (2-8 December 2005).

The average useful solar radiation (from sunrise to sunset) was equal to about 520 W m^{-2} for June and about 250 W m^{-2} for December; while the daily average ambient temperatures were 23.2 °C and 14.2 °C, respectively.

4.2 Results and comments

In Fig. 6a-b, the calculated temperatures of the solar collector, the adsorbent material and the condenser are presented. The solar collector temperatures had a daily maximum which ranges from 70 to about 105 °C in June, and from about 25 to 50 °C in December. The temperature of the adsorbent material was about 5 °C lower; this gradient depends on the thermal resistance between the solar collector and the adsorbent material. The maximum condenser temperature was about 30 °C in summer and 20 °C in winter. It is worthy to note that the first day of the week of December, which was very cold and weakly insulated, did not allow sufficient heating of the sorbent bed.

Figure 7a-b shows the adsorbent pressure and the corresponding values of methanol uptake of the adsorbent bed. In particular, the mean uptake is about 15% in June, and about 30% in December. It can be observed that, during the most sunny days (i.e. in June), uptake variations (daily gradients) greater than 10% were obtained; while, in December this value was about 5 % (with the exception of the first day of the week, in which the ambient conditions were unfavourable).

In Fig. 8a-b the behaviour of the temperature of methanol inside the evaporator and that of the mass of water converted to ice, in the cold chamber, are shown. It can be observed that in June (Fig. 8a) the system was able to produce 5 kg of ice, each day, at a temperature between –4 °C and –18 °C, which demonstrates a noticeable under-cooling of the ice. The same conclusion cannot be drawn for December; in this case there was a day (2 December) with no ice production and other days, characterized by a low solar energy available (3, 7-8 December), where the Daily Ice Production ranged between 2

and 4 kg. The temperature of the water in the cold chamber (not shown in Fig. 8a-b) is almost coincident with the evaporator temperature, due to the good thermal contact between liquid methanol and water.

Figure 9a-b shows the calculated COPs, DIP and DIP_{eq} for the considered periods. The average value of COPs in June was 0.052, with a maximum of 0.073. The amount of solar energy available exceeded the energy required for freezing the 5 kg of water; so that, the resulting values of DIP_{eq} ranged between 5.1 and 5.45 kg.

In December, the average and maximum COPs were 0.092 and 0.144, respectively. In this case, the amount of solar energy available is sufficient to produce a certain amount of ice (5 kg during favourable days), while the under-cooling of the ice is absent, as confirmed by the values of evaporator temperature and the equivalence between DIP and DIP_{eq} (see Figs. 8b and 9b).

Finally, in Fig. 10 the average monthly values of COPs, DIP and DIP_{eq}, calculated for the whole year 2005, are represented. The average COPs varies from a minimum of about 0.045 (July) to a maximum of 0.11 (January), with an annual mean of 0.07. The Daily Ice Production ranges from 2.07 (December) to 5 kg (from April to August), with an annual mean of 4.25 kg. In particular, the figure demonstrates that the targeted 5 kg of DIP can be obtained for about two-third of the year (i.e. from April to October). Besides, in some months (from April to September, excluding July), a further equivalent amount of ice, up to a maximum of 0.5 kg (May), is associated to the under-cooling effect (maximum and annual mean DIP_{eq} are 5.5 kg and 4.45 kg, respectively).

During the months of February and March the average monthly DIP is about 4 kg, while the DIP_{eq} values are slightly higher (4.47 kg, on March). This depends on the fact that for several days the ice-maker is still able to produce 5 kg of ice. Worse performance are obtained for the coldest months of the year (January, November and December), when the calculated DIP values (2.0-3.5 kg) are lower than the targeted value.

DIP and COPs values derived from the present model are in agreement with those reported in literature. In particular, a solar COP in the order of 0.10-0.14 and a daily ice production in the order of 4-5 kg m^{-2} are often reported as typical for ice-makers based on the activated carbon/methanol pair [3-5, 8, 11, 13, 15]. These values are coherent with those calculated by our model (Figs. 9-10) for some days. However, our study evidenced that the COPs and DIP values may be significantly affected when the climatic conditions are not favourable. This is also confirmed by some analyses carried out on a solar ice-maker with activated carbon/methanol adsorption pair tested in Kunming, China [22]: its DIP varies in the range 3.2-6.5 kg m^{-2} and the solar COP is 0.083-0.127; but, there are also two days with "no ice production" (DIP=0) and COP equal to about 0.03. These results, previously reported in literature, represent a preliminary validation of the proposed model, which should be definitely accomplished when the measured performance parameters of a prototype will be available.

5. Conclusions

A dynamic model for simulation and study of an adsorptive ice-maker is presented. The model was firstly applied to typical representative summer (June) and winter (December) conditions, considering climatic data of Messina. Furthermore, simulations for the whole year 2005 have been performed.

The simulation results demonstrated that the design of the proposed ice-maker allows to provide a Daily Ice Production of 5 kg, or slightly lower, for the most part of the year (from April to October). While, lower amounts of ice are obtained in the remaining months of the year: about 4 kg in February and March; between 2.0 and 3.5 kg in the coldest months (January, November and December). The average monthly COPs varies from a minimum of about 0.045 (July) to a maximum of 0.11 (January), with an annual mean of 0.07.

Further performance improvements can be achieved through the optimization of the system design and, in particular, by enhancing the heat transfer between the solar collector and the adsorber and/or by using adsorbent materials with higher sorption ability, compared to the active carbon.

References

[1] Critoph RE. Performance limitations of adsorption cycles for solar cooling. Solar Energy 1988; 41 (1), 21-31.

[2] Dieng A, Wang RZ. Literature review on solar adsorption technologies for ice-making and air-conditioning purposes and recent developments in solar technology. Renewable & Sustainable Energy Reviews 2001; 5, 313-42.

[3] Sumathy K, Li Zhongfu F. Experiments with solar-powered adsorption ice-maker. Renewable Energy 1998; 16, 704-7.

[4] Li ZF, Sumathy K. A solar powered ice-maker with the solid adsorption pair of activated carbon and methanol. International Journal of Energy Research 1999; 23, 517-27.

[5] Li M, Wang RZ, Xu Y, Wu J, Dieng A. Experimental study on dynamic performance analysis of a flat-plate solar solid-adsorption refrigeration for ice maker. Renewable Energy 2002; 27, 211-21.

[6] Anyanwu EE, Ezekwe CI. Design, construction and test run of a solid adsorption solar refrigerator using activated carbon/methanol, as adsorbent/adsorbate pair. Energy Conversion & Management 2003; 44, 2879-92.

[7] Hildbrand C, Dind P, Pons M, Buchter F. A new solar powered adsorption refrigerator with high performance. Solar Energy 2004; 77 (3), 311-18.

[8] Passos EF, Escobedo JF, Meunier F. Simulation of an intermittent adsorptive solar cooling system. Solar Energy 1989; 42 (2), 103-11.

[9] Hu EJ. Simulated results of a non-valve, daily-cycled, solar-powered carbon/methanol refrigerator with a tubular solar collector. Applied Thermal Engineering 1996; 16 (5), 439-45.

[10] Anyanwu EE, Oteh UU, Ogueke NV. Simulation of a solid adsorption solar refrigerator using activated carbon/methanol adsorbent/refrigerant pair. Energy Conversion & Management 2001; 42, 899-915.

[11] Li M, Wang RZ. Heat and mass transfer in a flat plate solar solid adsorption refrigeration ice maker. Renewable Energy 2003; 28 (4), 613-22.

[12] Dai YJ, Sumathy K. Heat and mass transfer in the adsorbent of a solar adsorption cooling system with glass tube insulation. Energy 2003; 28, 1511-27.

[13] Leite A, Daguenet M. Performance of a new solid adsorption ice maker with solar energy. Energy Conversion & Management 2000; 41, 1625-47.

[14] Hu EJ, Exell RHB. Simulation and sensitivity analysis of an intermittent solar powered charcoal/methanol refrigerator. Renewable Energy 1994; 4 (1), 133-49.

[15] Boubakri A, Guilleminot J, Meunier F. Adsorptive solar powered ice-maker: experiments and model. Solar Energy 2000; 69 (3), 249-63.

[16] Cacciola G, Restuccia G. Reversible adsorption heat pump: a thermodynamic model. International Journal of Refrigeration 1995; 18 (2), 100-6.

[17] Rohsenow WM, Hartnett JP, Ganić. Handbook of Heat Transfer Applications, Second Edition. McGraw-Hill, New York, 1985, p. 4-4.

[18] Restuccia G, Aristov YI, Maggio G, Cacciola G, Tokarev MM. Performance of sorption systems using new selective water sorbents. Proceedings of the International Sorption Heat Pump Conference (ISHPC), pp. 219-23, Munich, Germany, March 24-26, 1999.

[19] Zanifé T. “Etude d’une pompe à chaleur de 230 kW et d’une machine frigorifique à adsorption solide”, PhD Thesis, n° 91 PA06 6390, University of Paris VI, Paris, France (1991).

[20] Wolfram S. The Mathematica Book, Fourth Edition, Mathematica Version 4. Wolfram Media and Cambridge University Press, Cambridge, 1999.

[21] Radhakrishnan K, Hindmarsh AC. Description and Use of LSODE, the Livermore Solver for Ordinary Differential Equations, Lawrence Livermore National Laboratory technical report UCRL-ID-113855, March 1994.

[22] Luo HL, Dai YJ, Wang RZ, Tang R, Li M. “Year round test of a solar adsorption ice maker in Kunming, China”. Energy Conversion and Management 2005; 46 (13-14), 2032-41.

FIGURE CAPTIONS:

Figure 1: Scheme of the adsorptive ice-maker.

Figure 2: Ideal adsorption cycle in the Clapeyron diagram.

Figure 3: Control volume for modeling. 1: Solar collector; 2: Metallic housing of the adsorbent bed; 3: Adsorbent bed; 4: Condenser; 5: Water/ice: 6: Evaporator/water (ice) interface; 7: Evaporator.

Figure 4: Design of the ice-maker (left) and solar collector (right).

Figure 5a,b: Solar radiation and ambient temperature recorded in June (top) and December 2005 (bottom).

Figure 6a,b: Adsorbent material, solar collector and condenser temperature calculated for June (top) and December 2005 (bottom).

Figure 7a,b: Methanol uptake and adsorbent pressure calculated for June (top) and December 2005 (bottom).

Figure 8a,b: Evaporator temperature and mass of ice calculated for June (top) and December 2005 (bottom).

Figure 9a,b: COPs, DIP and DIP_{eq} calculated for June (top) and December 2005 (bottom).

Figure 10: Monthly average COPs, DIP and DIP_{eq} calculated for the whole year 2005.

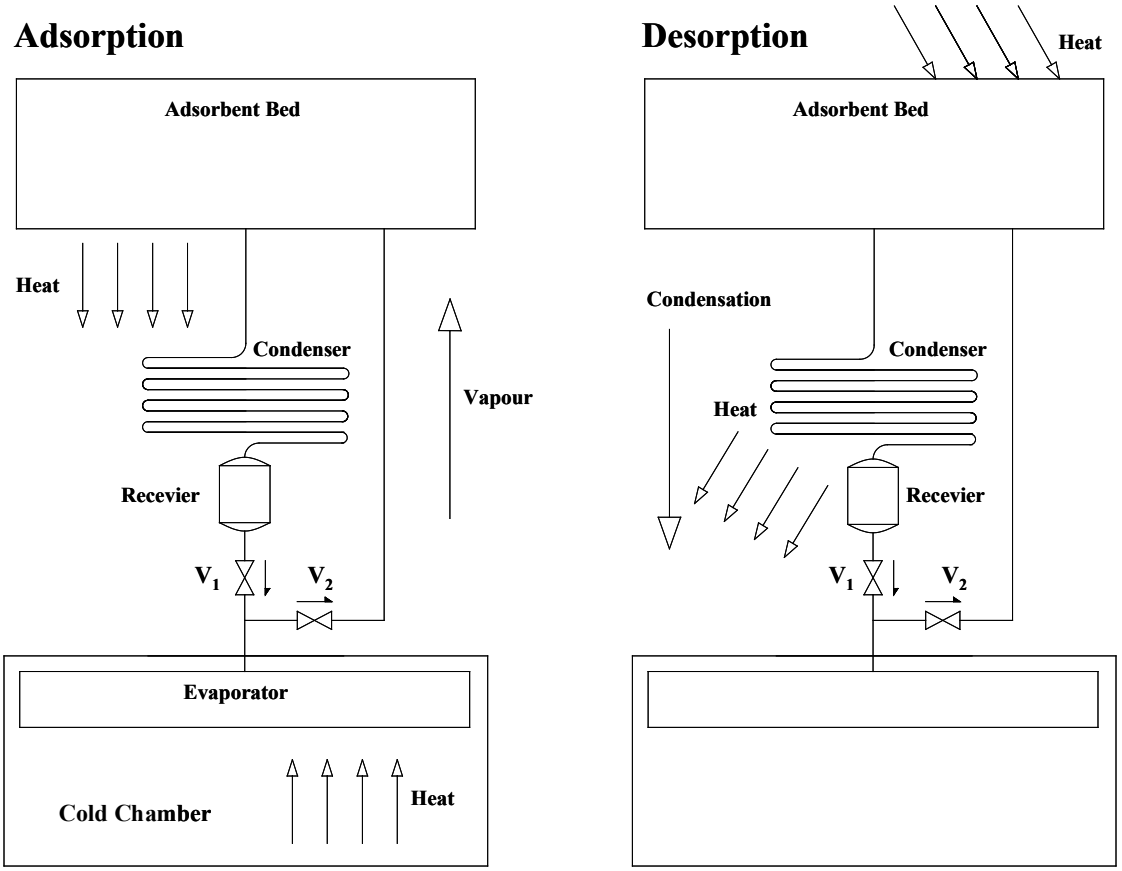
Adsorption
Adsorbent Bed
Heat
Condenser
Vapour
Recevier
V1
V2
Evaporator
Cold Chamber
Heat
Desorption
Heat
Adsorbent Bed
Condensation
Condenser
Heat
Recevier
V1
V2

Figure 1

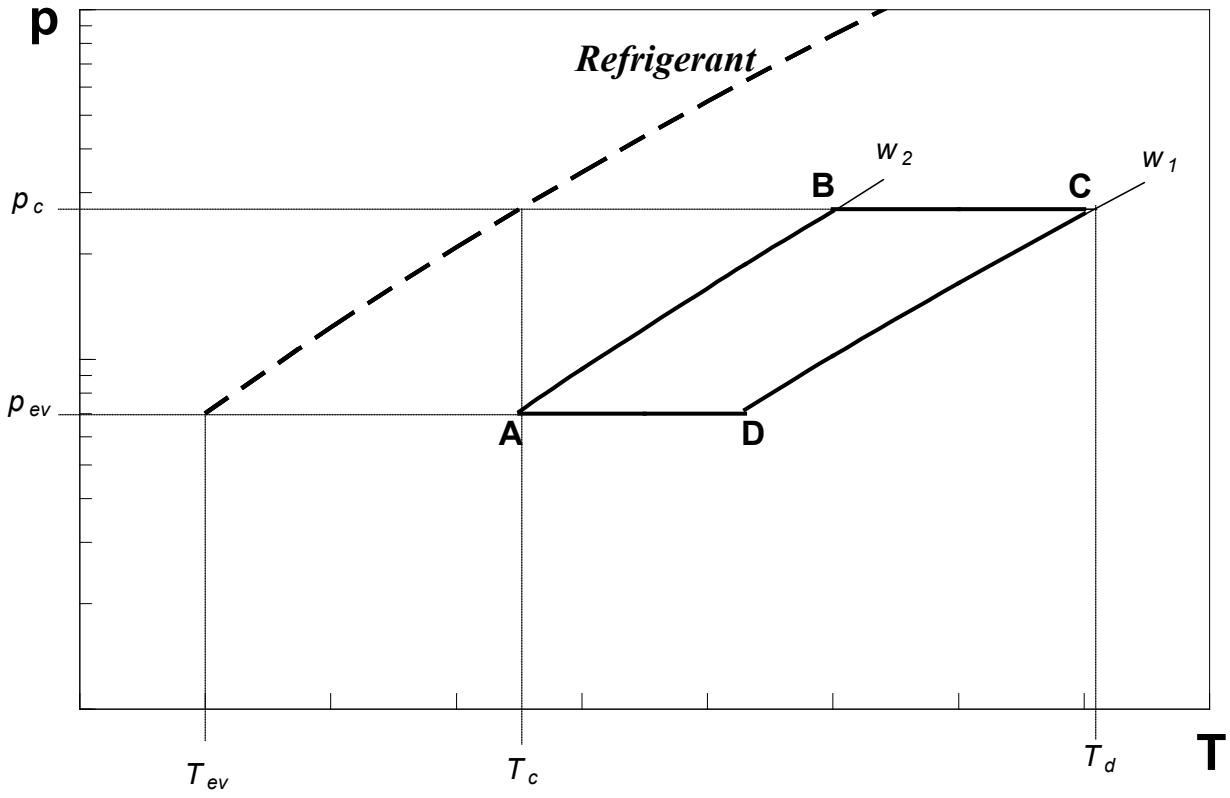

Figure 2

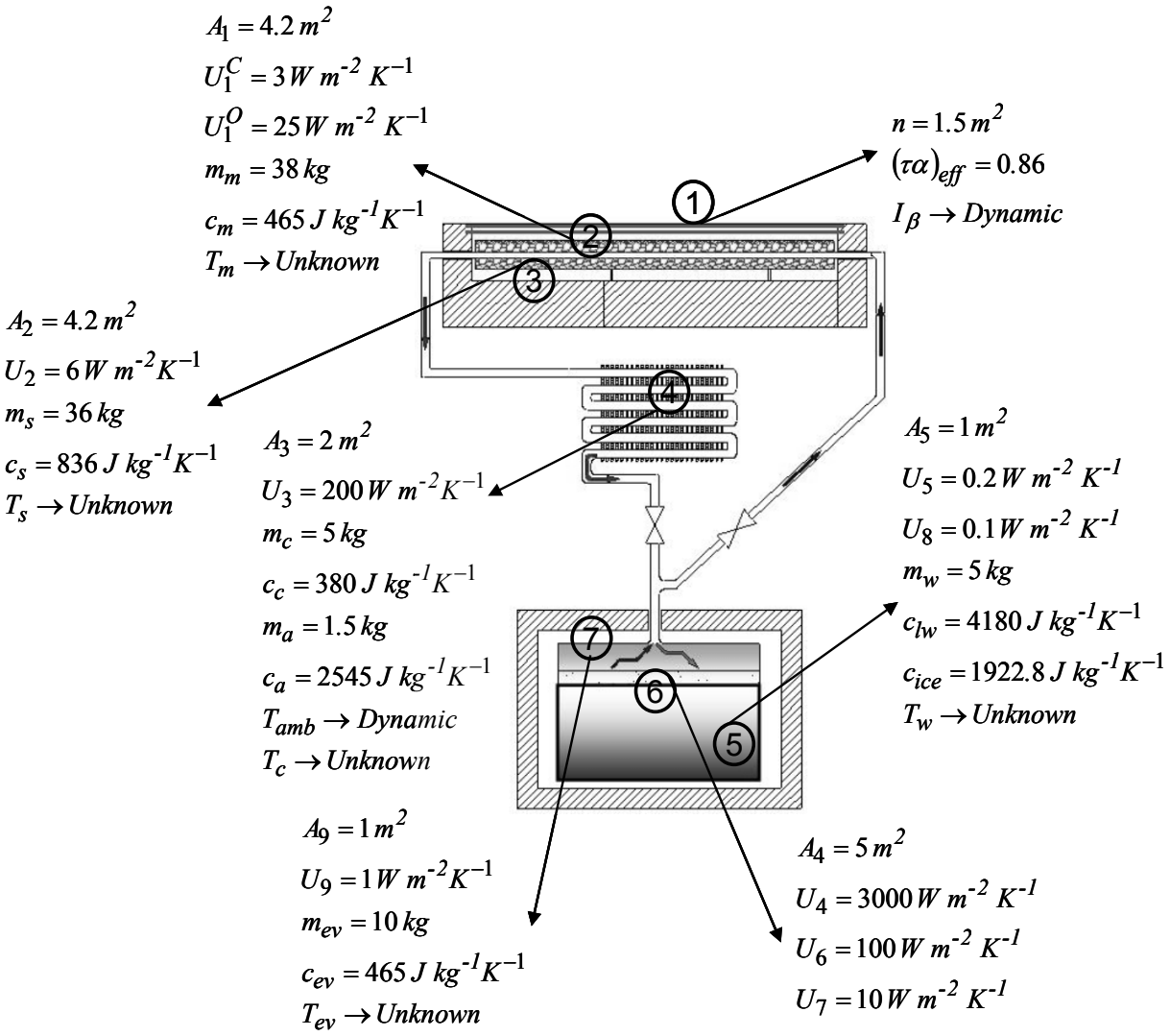
$A_1 = 4.2\,m^2$
$U_1^C = 3\,W\,m^{-2}\,K^{-1}$
$U_1^O = 25\,W\,m^{-2}\,K^{-1}$
$m_m = 38\,kg$
$c_m = 465\,J\,kg^{-1}K^{-1}$
$T_m \rightarrow Unknown$
$n = 1.5\,m^2$
$(\tau\alpha)_{eff} = 0.86$
$I_\beta \rightarrow Dynamic$
$A_2 = 4.2\,m^2$
$U_2 = 6\,W\,m^{-2}K^{-1}$
$m_s = 36\,kg$
$c_s = 836\,J\,kg^{-1}K^{-1}$
$T_s \rightarrow Unknown$
$A_3 = 2\,m^2$
$U_3 = 200\,W\,m^{-2}K^{-1}$
$m_c = 5\,kg$
$c_c = 380\,J\,kg^{-1}K^{-1}$
$m_a = 1.5\,kg$
$c_a = 2545\,J\,kg^{-1}K^{-1}$
$T_{amb} \rightarrow Dynamic$
$T_c \rightarrow Unknown$
$A_5 = 1\,m^2$
$U_5 = 0.2\,W\,m^{-2}\,K^{-1}$
$U_8 = 0.1\,W\,m^{-2}\,K^{-1}$
$m_w = 5\,kg$
$c_{lw} = 4180\,J\,kg^{-1}K^{-1}$
$c_{ice} = 1922.8\,J\,kg^{-1}K^{-1}$
$T_w \rightarrow Unknown$
$A_9 = 1\,m^2$
$U_9 = 1\,W\,m^{-2}K^{-1}$
$m_{ev} = 10\,kg$
$c_{ev} = 465\,J\,kg^{-1}K^{-1}$
$T_{ev} \rightarrow Unknown$
$A_4 = 5\,m^2$
$U_4 = 3000\,W\,m^{-2}\,K^{-1}$
$U_6 = 100\,W\,m^{-2}\,K^{-1}$
$U_7 = 10\,W\,m^{-2}\,K^{-1}$
1
2
3
4
5
6
7

Figure 3

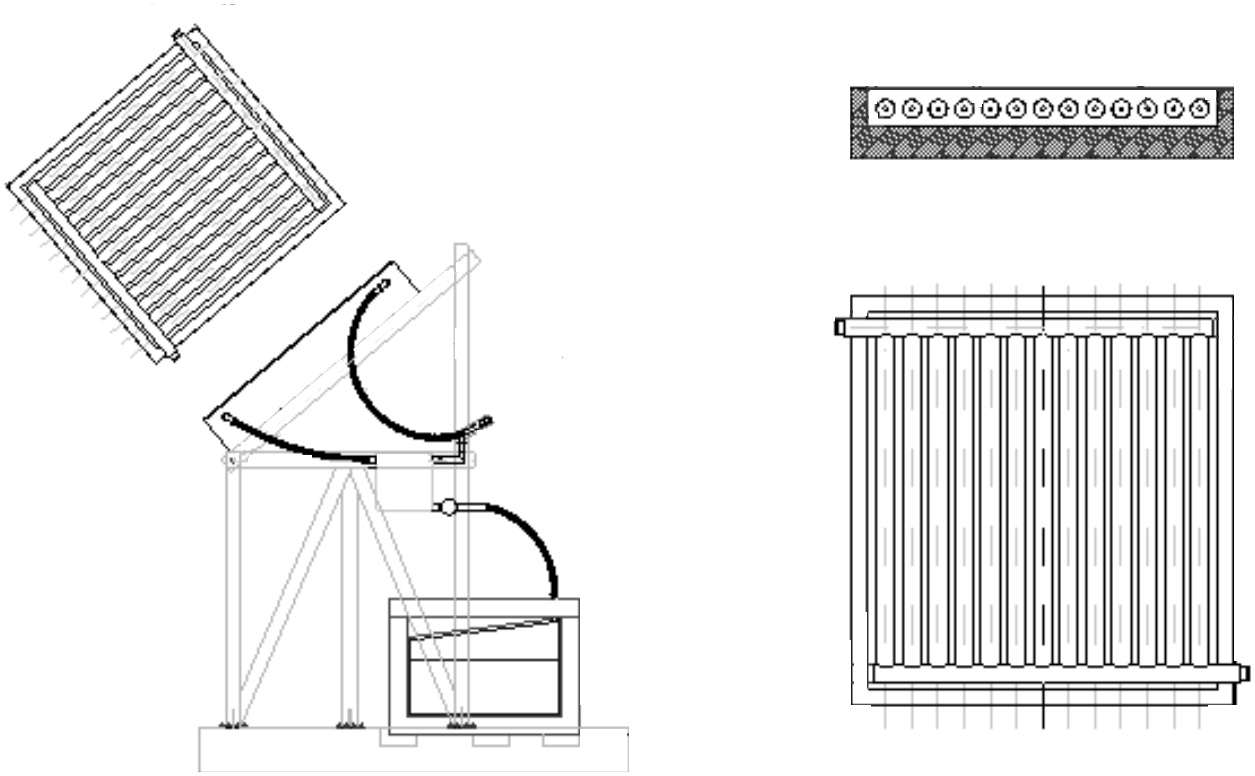

Figure 4

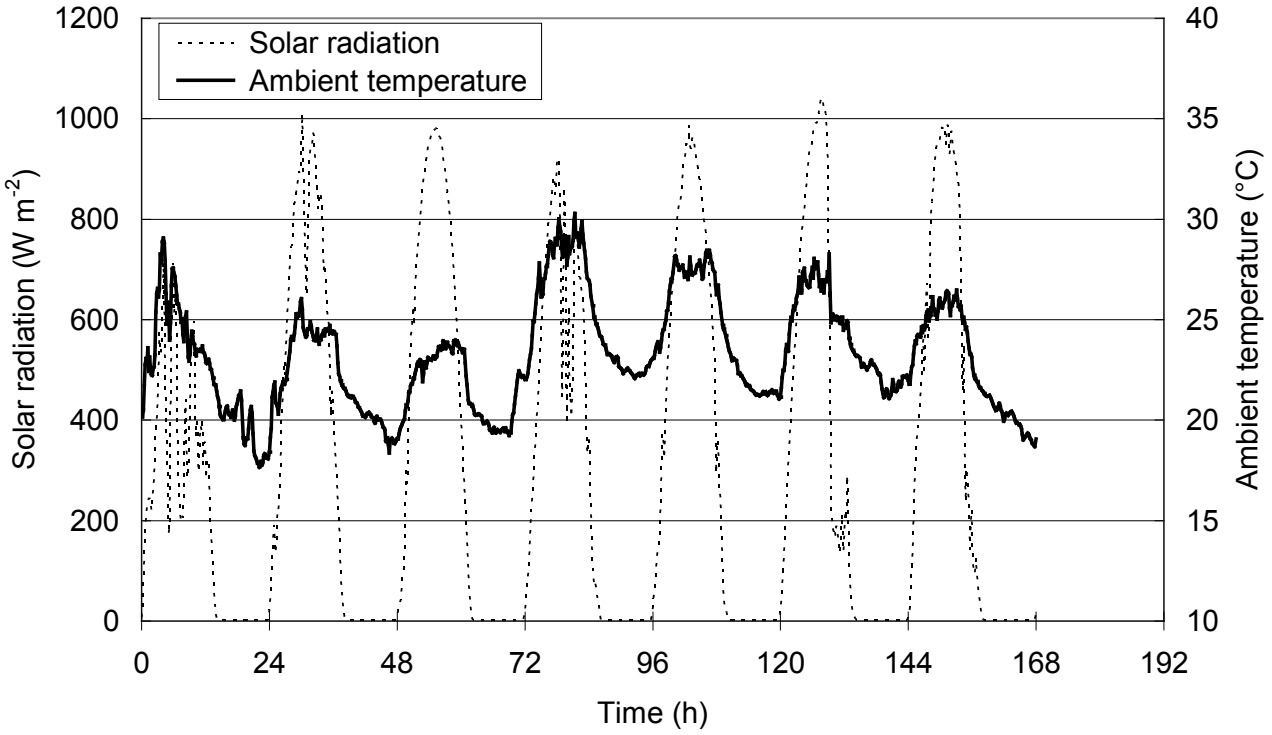
Solar radiation
Ambient temperature
Solar radiation (W m-2)
Ambient temperature (°C)
Time (h)
0
200
400
600
800
1000
1200
10
15
20
25
30
35
40
0
24
48
72
96
120
144
168
192

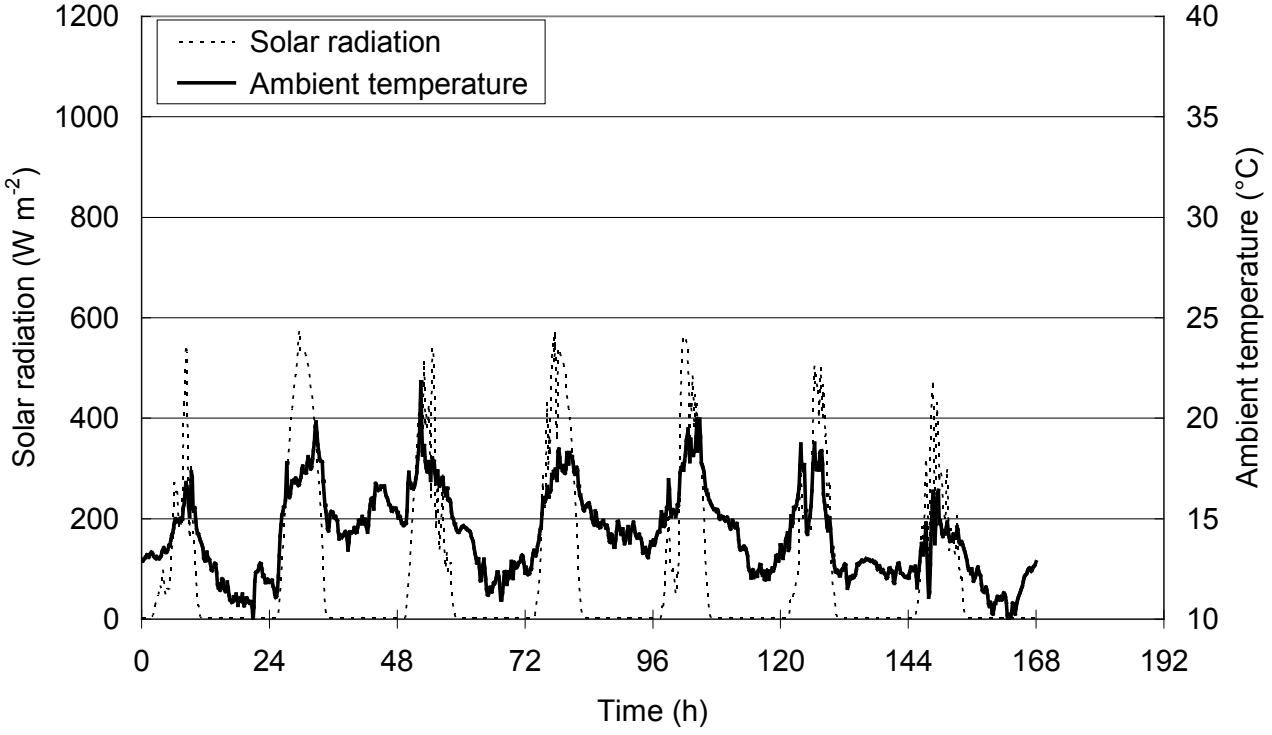
Solar radiation
Ambient temperature
Solar radiation (W m-2)
Ambient temperature (°C)
Time (h)
0
200
400
600
800
1000
1200
10
15
20
25
30
35
40
0
24
48
72
96
120
144
168
192

Figure 5a,b

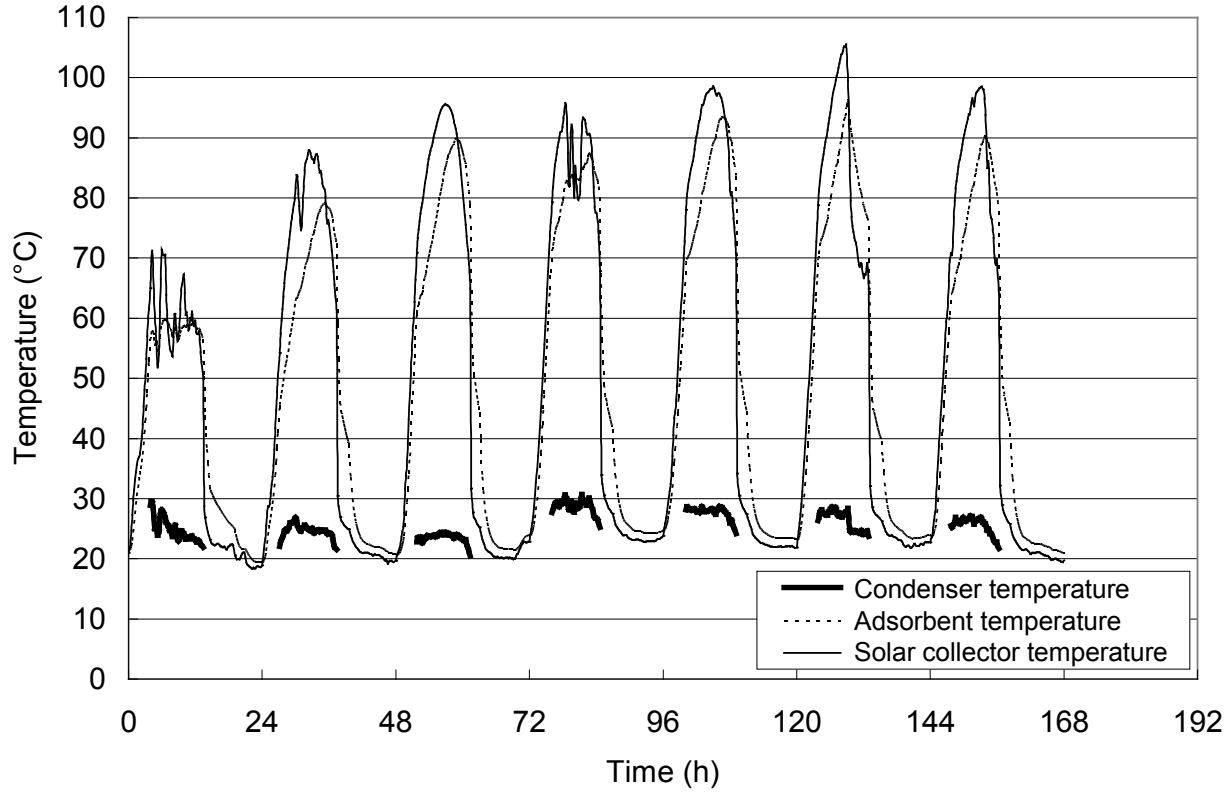
Temperature (°C)
Time (h)
Condenser temperature
Adsorbent temperature
Solar collector temperature

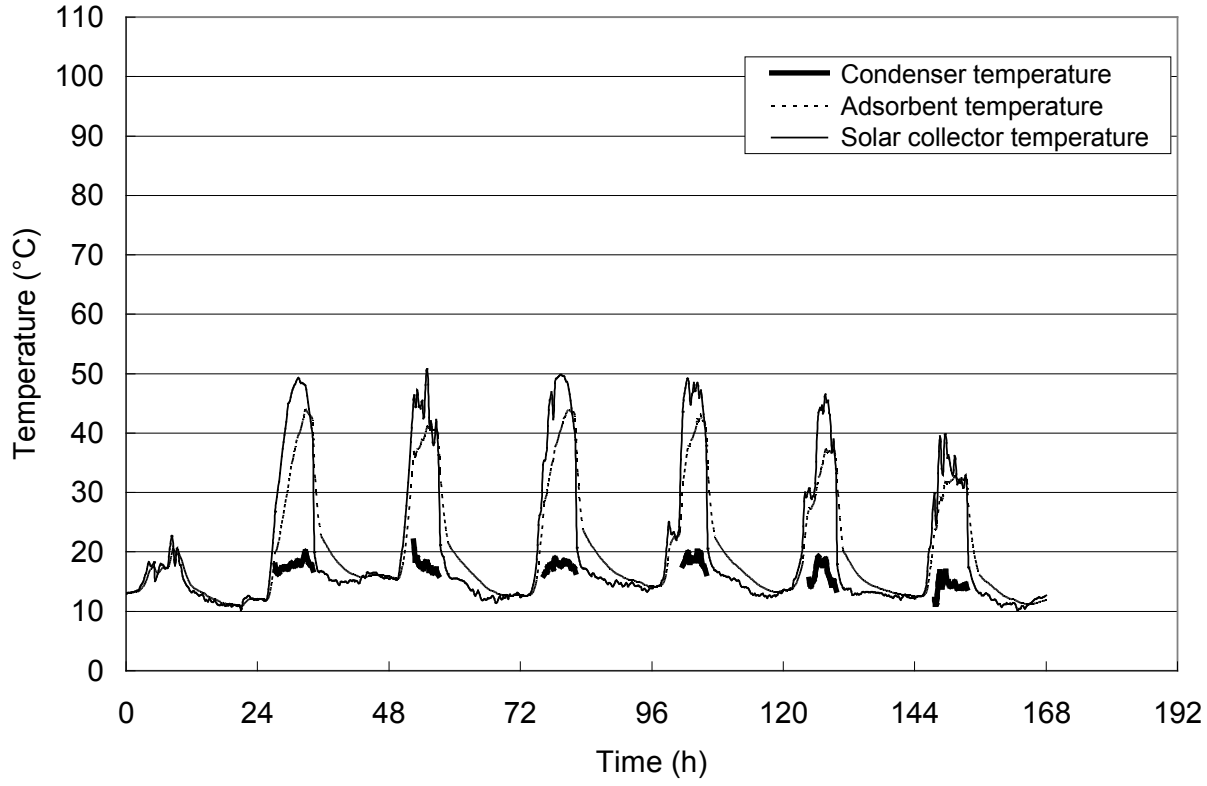
Temperature (°C)
Time (h)
Condenser temperature
Adsorbent temperature
Solar collector temperature

Figure 6a,b

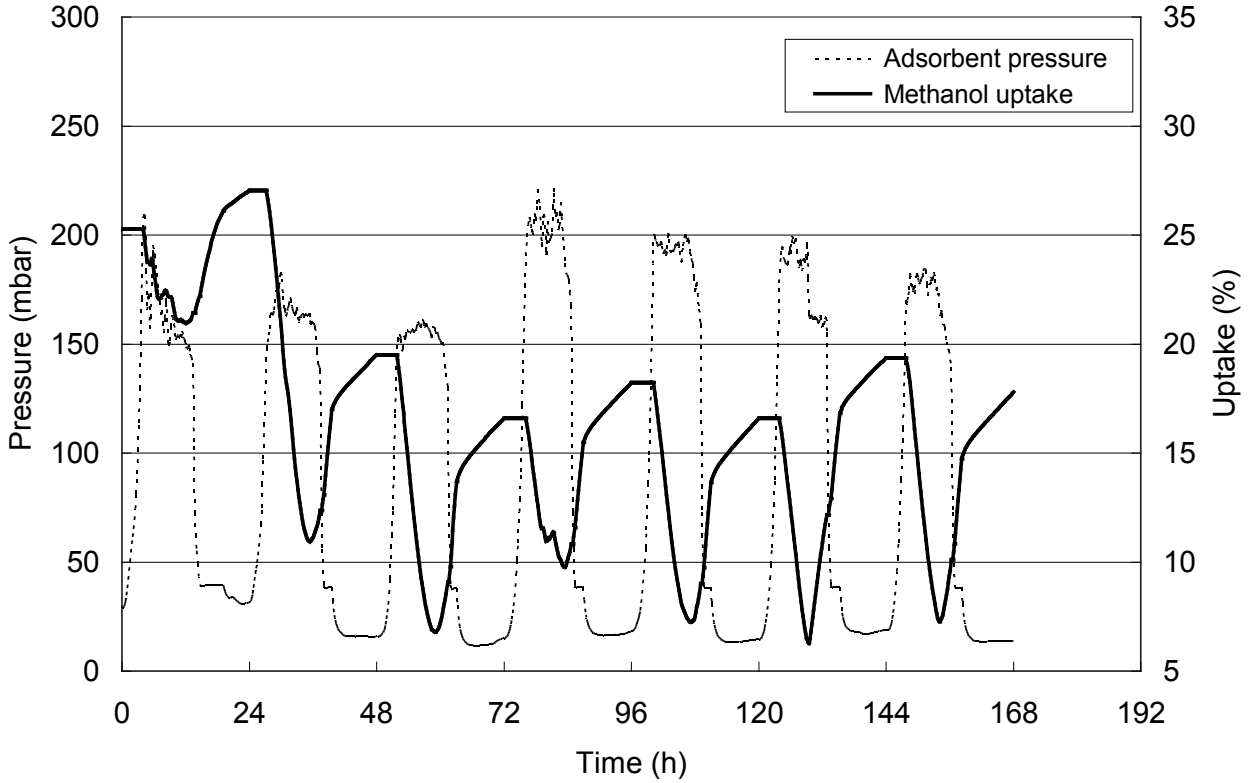
Adsorbent pressure
Methanol uptake
Pressure (mbar)
Uptake (%)
Time (h)
0
50
100
150
200
250
300
5
10
15
20
25
30
35
0
24
48
72
96
120
144
168
192

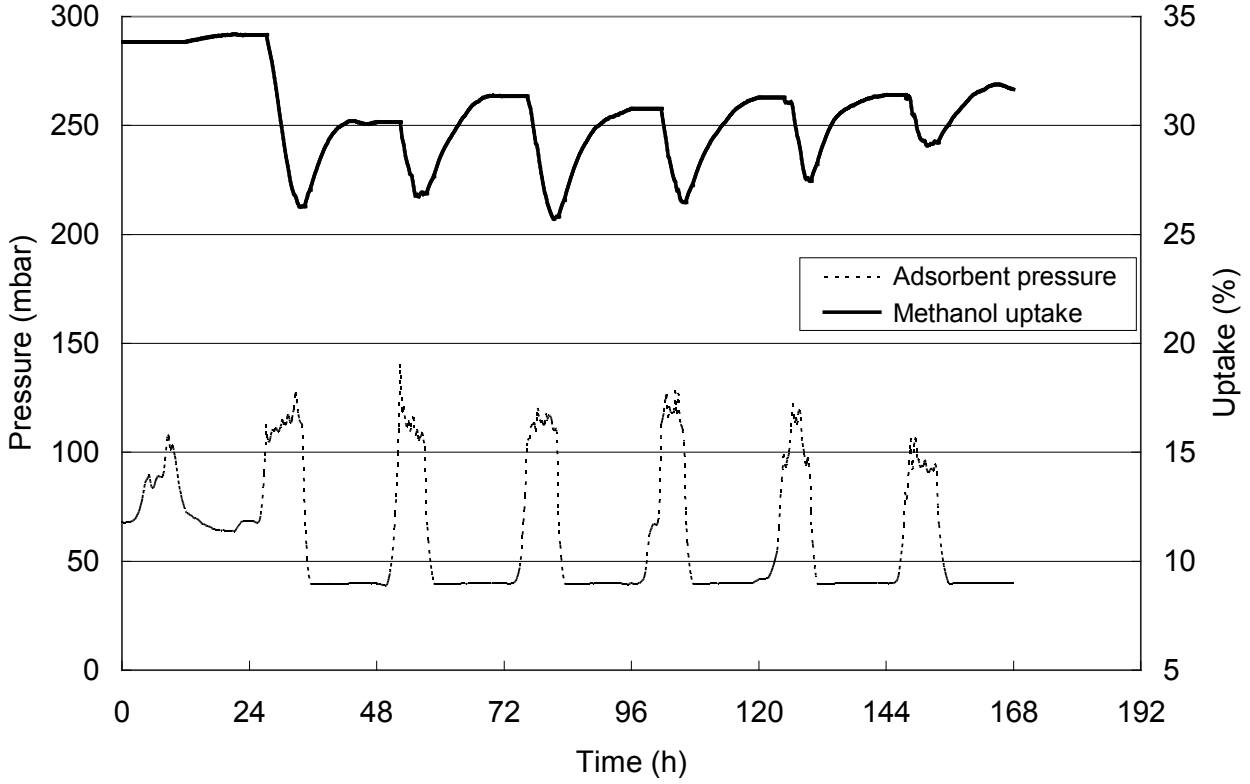
Adsorbent pressure
Methanol uptake
Pressure (mbar)
Uptake (%)
Time (h)
0
50
100
150
200
250
300
5
10
15
20
25
30
35
0
24
48
72
96
120
144
168
192

Figure 7a,b

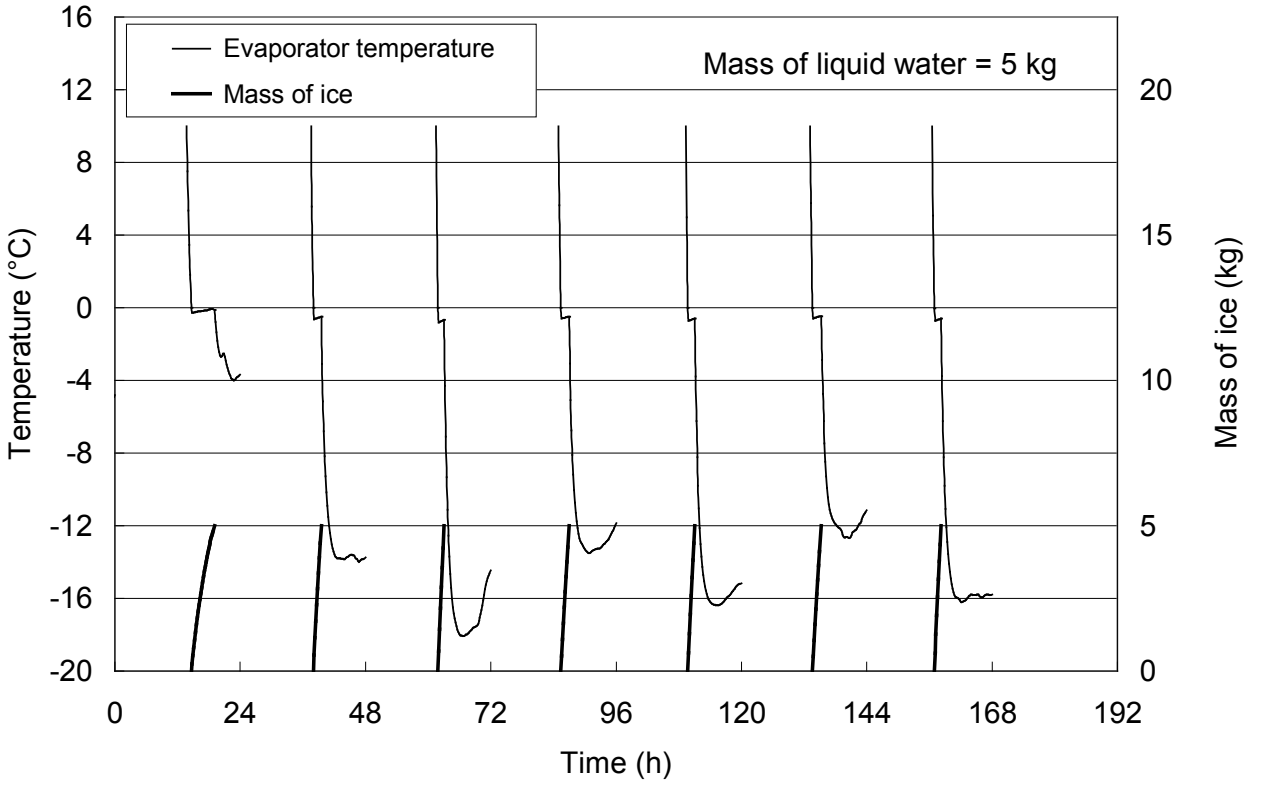
Evaporator temperature
Mass of ice
Mass of liquid water = 5 kg
Temperature (°C)
Mass of ice (kg)
Time (h)
16
12
8
4
0
-4
-8
-12
-16
-20
20
15
10
5
0
0
24
48
72
96
120
144
168
192

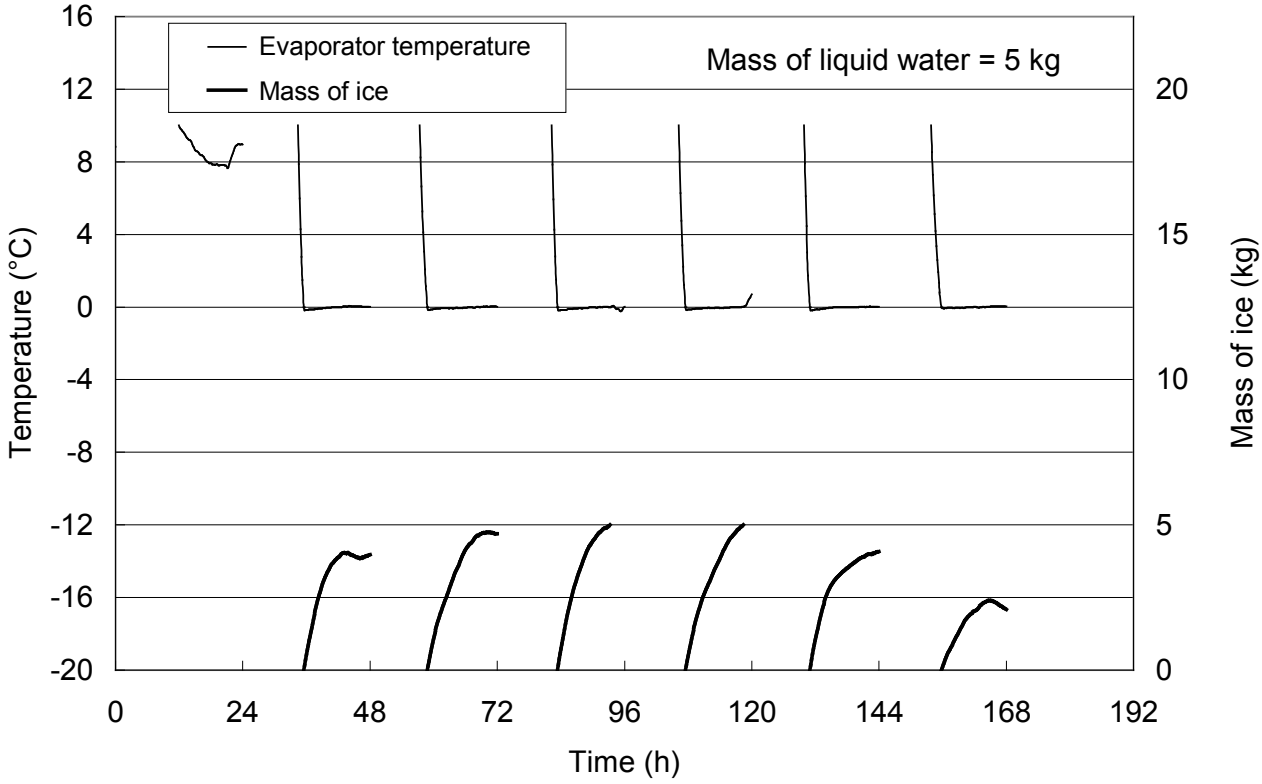
Evaporator temperature
Mass of ice
Mass of liquid water = 5 kg
Temperature (°C)
Mass of ice (kg)
Time (h)
16
12
8
4
0
-4
-8
-12
-16
-20
20
15
10
5
0
0
24
48
72
96
120
144
168
192

Figure 8a,b

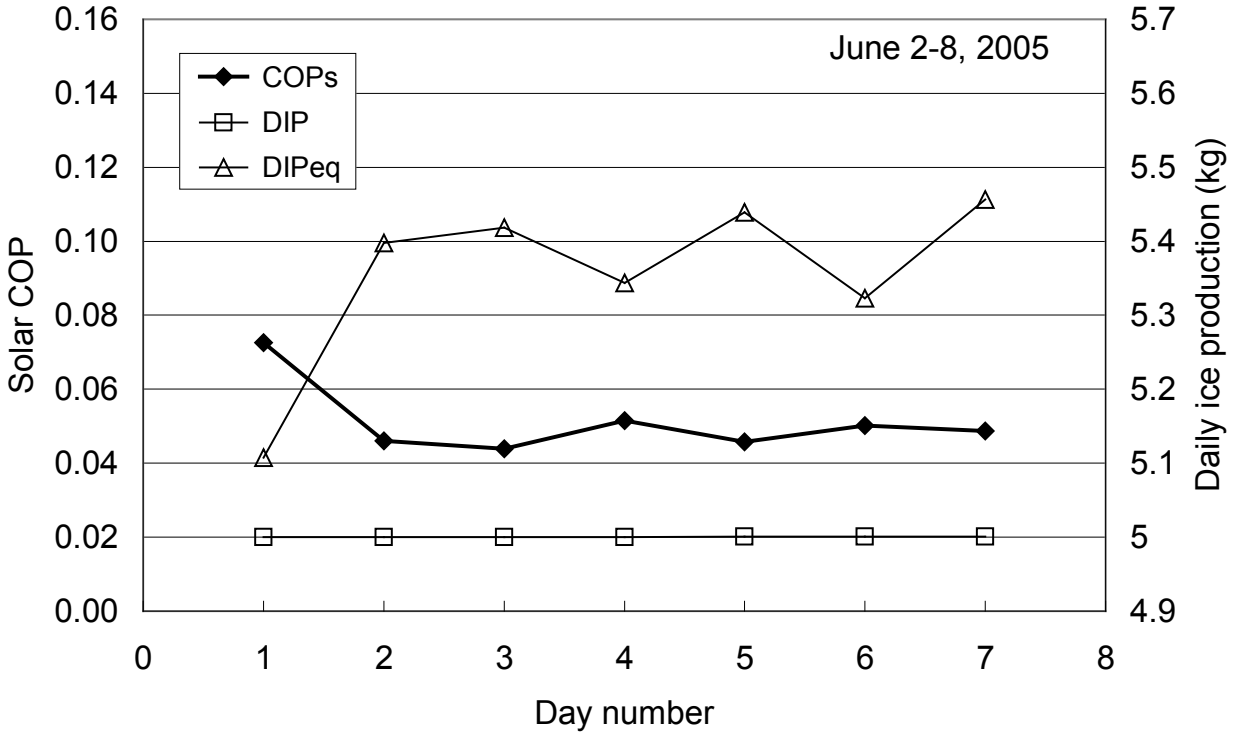
June 2-8, 2005
COPs
DIP
DIPeq
Solar COP
Daily ice production (kg)
Day number
0.16
0.14
0.12
0.10
0.08
0.06
0.04
0.02
0.00
5.7
5.6
5.5
5.4
5.3
5.2
5.1
5
4.9
0
1
2
3
4
5
6
7
8

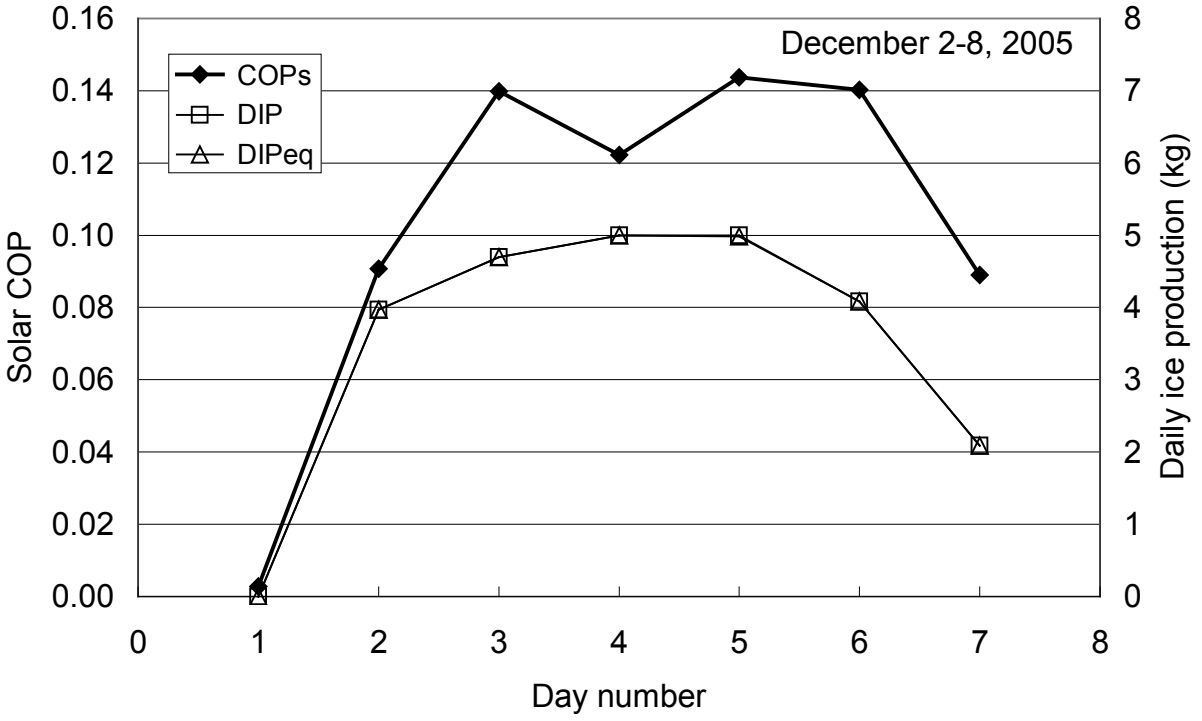
December 2-8, 2005
COPs
DIP
DIPeq
Solar COP
Daily ice production (kg)
Day number
0.16
0.14
0.12
0.10
0.08
0.06
0.04
0.02
0.00
8
7
6
5
4
3
2
1
0
0
1
2
3
4
5
6
7
8

Figure 9a,b

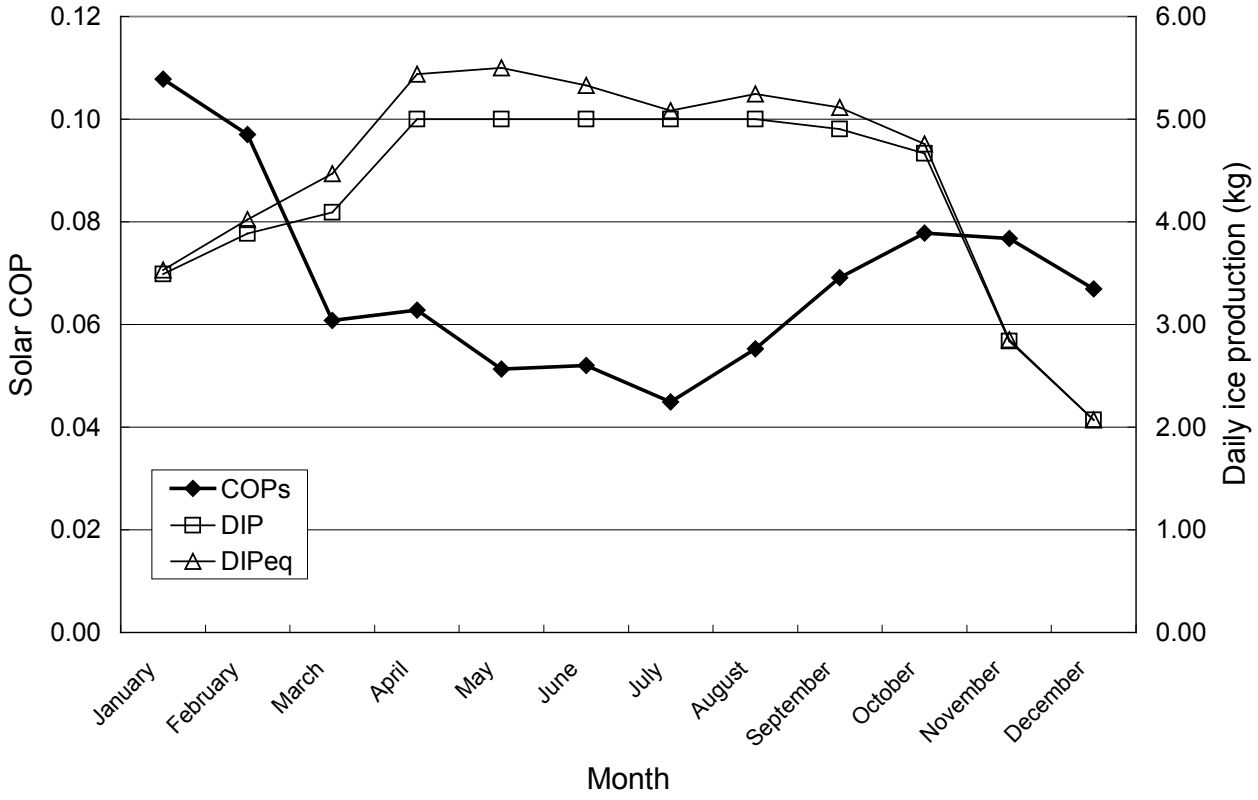
0.12
0.10
0.08
0.06
0.04
0.02
0.00
Solar COP
6.00
5.00
4.00
3.00
2.00
1.00
0.00
Daily ice production (kg)
COPs
DIP
DIPeq
January
February
March
April
May
June
July
August
September
October
November
December
Month

Figure 10

Table 1: Equations, Coefficients and End phase conditions for Phase I and III.

	Phase I	Phase III
Equations	Eq. (1) Eq. (2) Eq. (7)	
Coefficents	K_1=0	
	$U_1^{C/O} = U_1^{C}$	$U_1^{C/O} = U_1^{O}$
End phase condition	p_s=p_c	p_s=p_{ev}

Table 2: Equations, Coefficients and End phase conditions for Phase II and IV.

	Phase II	Phase IV		
		Step a	Step b	Step c
Equations		Eq. (1) Eq. (2) Eq. (7)		
	Eq. (3a) Eq. (11a)		Eq. (3b) Eq. (11b)	
		Eq. (4)	Eq. (5)	Eq. (4)
Coefficents		K_1=1		
	$U_1^{C/O} = U_1^C$		$U_1^{C/O} = U_1^O$	
		U_α=U_4, U_β=U_5, c_w=c_{lw}	U_α=U_6	U_α=U_7, U_β=U_8, c_w=c_{ice}
End phase condition	I_β<100 $W\,m^{-2}$ *or* $w \leq 2\%$	T_w=0 or *t= 24 h*	$m_{ice} = m_w$ or *t= 24 h*	*t= 24 h*